Electronic Supplementary Information

Ultrasensitive detection of nitro explosive-picric acid *via* conjugated polyelectrolyte in aqueous media and solid support

Sameer Hussain,[a] *Akhtar Hussain Malik,*[a] *Mohammad Adil Afroz,*[a] *and Parameswar Krishnan Iyer*[a,b]*

[a]Department of Chemistry, Indian Institute of Technology Guwahati, Guwahati-781039. India
[b]Centre for Nanotechnology, Indian Institute of Technology Guwahati, Guwahati, 781039, India

AUTHOR EMAIL ADDRESS: pki@iitg.ernet.in

AUTHOR FAX: +91 361 258 2349

Experimental Section

Caution! The nitroaromatics used in the study, especially picric acid, are highly explosives in nature and should be handled cautiously in small quantities with safety measures to avoid any explosion.

Materials and Methods

Nitroexplosives *viz.* 2, 6-DNT, 2, 4-DNT, 4-NT, 1, 3-DNB and chitosan were purchased from Aldrich Chemicals. Picric acid was purchased from Loba Chemie. All other chemicals and reagents and were purchased from Alfa-Aesar and Merck and were used without further purification. Milli-Q water was used in all the experiments. UV/visible spectra were recorded on a Perkin Elmer Lambda-25 spectrophotometer. Photoluminescence spectra were taken on a Horiba Fluoromax-4 spectrofluorometer using 10 mm path length quartz cuvettes with a slit width of 2 nm at 298 K. Electrochemical measurements were performed using a CH instruments Model 700D series Electrochemical workstation. Paper strip tests were performed using Whatman® qualitative filter paper, Grade 1. Time resolved fluorescence studies were performed in an Edinburgh Instruments Life Spec II instrument.

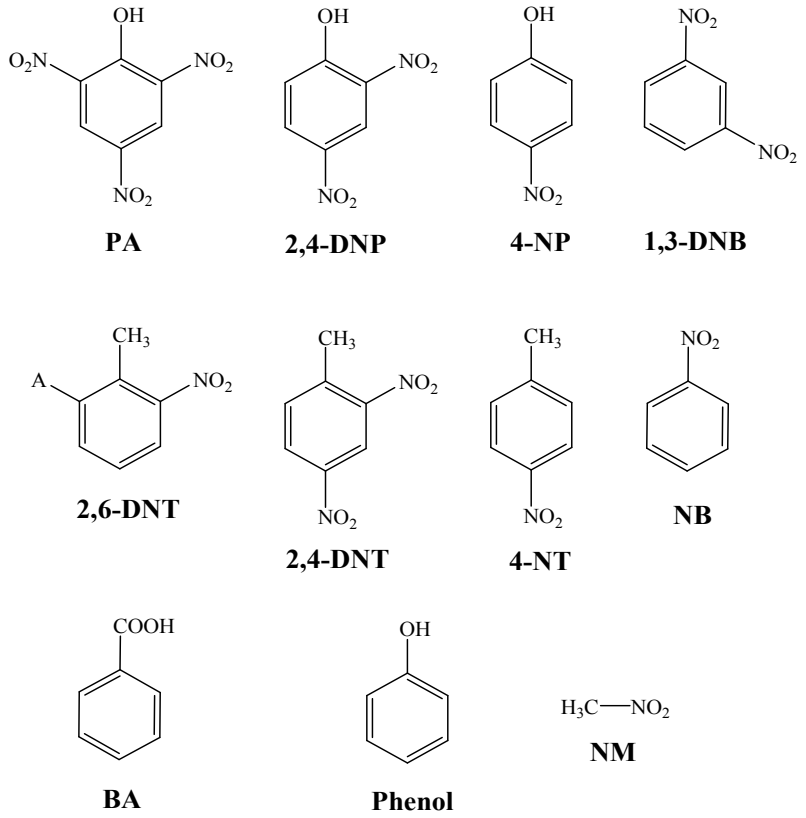

Scheme S1: Structures of various nitroexplosives and electron deficient compounds used in the experiments.

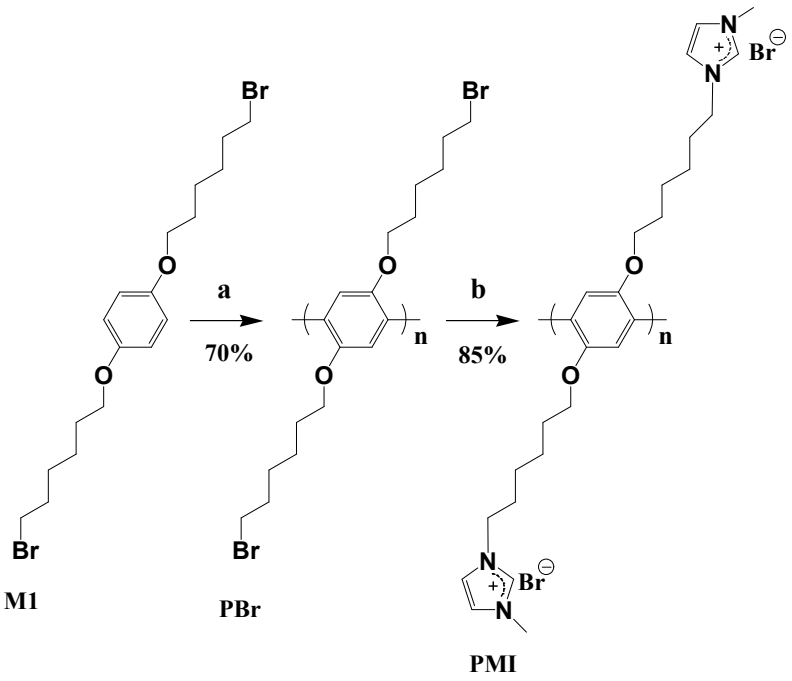

Scheme S2. (a) $FeCl_3$, nitrobenzene, RT, 36 hr (b) 1-methyl imidazole, reflux, 24 hr.

Synthesis of M1 and PBr

Synthesis of monomer M1 and polymer PBr was carried out using a previously established procedure.[1-3]

Synthesis of PMI

The polymer PMI was prepared according to the previously reported method.[4] In a 100mL round-bottom flask, PBr (0.12 mmol, 1eq.) and excess 1-methyl imidazole were taken and kept for reflux under stirring condition in an oil bath at 80ºC for 24 hours. The reaction mixture was then poured into excess chloroform and stirred for 1 hr to get precipitate. The process was repeated twice to remove excess 1-methyl imidazole and PBr. The precipitate was then filtered out and dried to obtain brownish colored product. Yield: 85%

^{1}H NMR (600 MHz, DMSO-*d6*, δ): 9.38 (b, 2H), 7.75 (b, 2H), 7.69 (b, 2H), 7.02 (b, 2H), 4.18 (b, 2H), 3.87 (b, 10H), 1.90 (b, 4H), 1.76 (b, 4H), 1.29 (b, 4H), 1.24 (b, 4H).

^{13}C NMR (150 MHz, DMSO-*d6*, δ): 149.47, 136.50, 128.64, 123.50, 122.25, 114.20, 68.73, 48.69, 35.78, 29.79, 28.70, 28.49, 25.53.

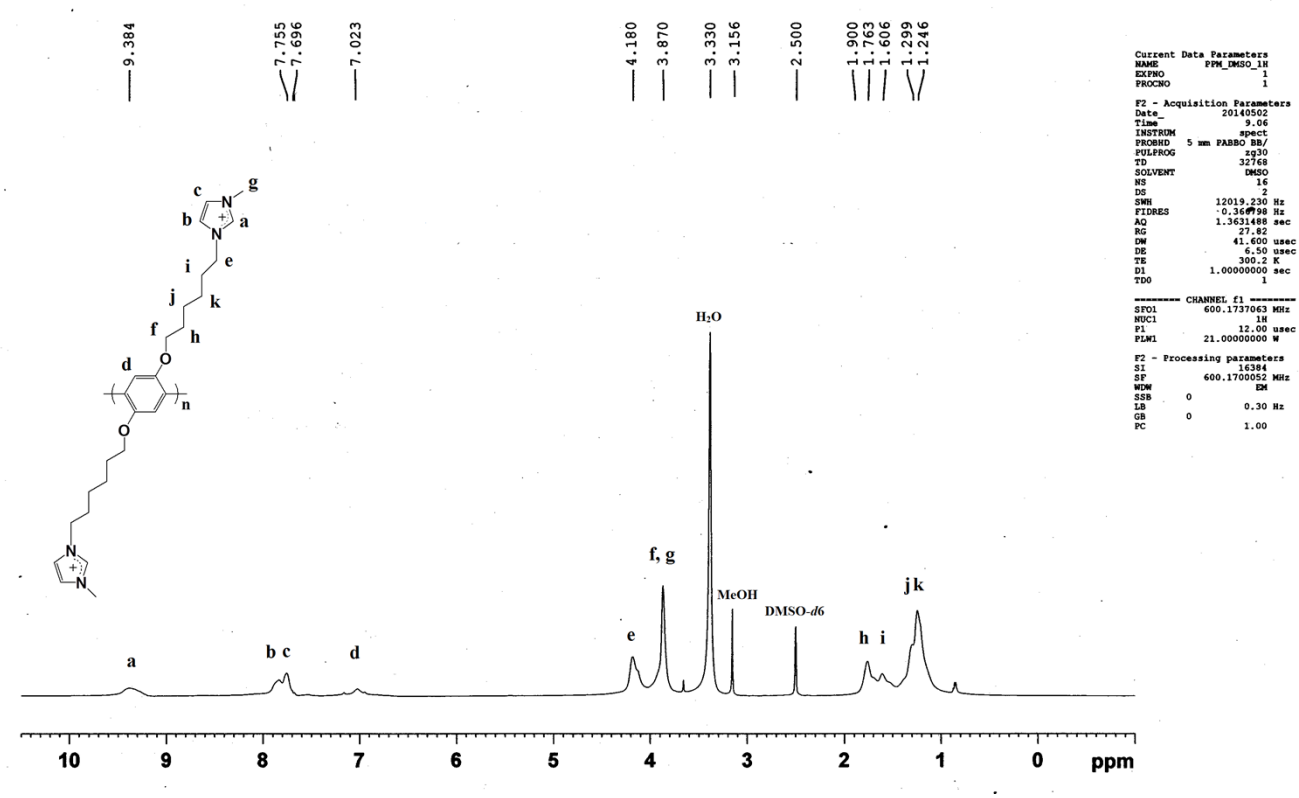

Fig. S1 ^{1}H NMR (600MHz, DMSO-*d6*) spectrum of PMI**.**

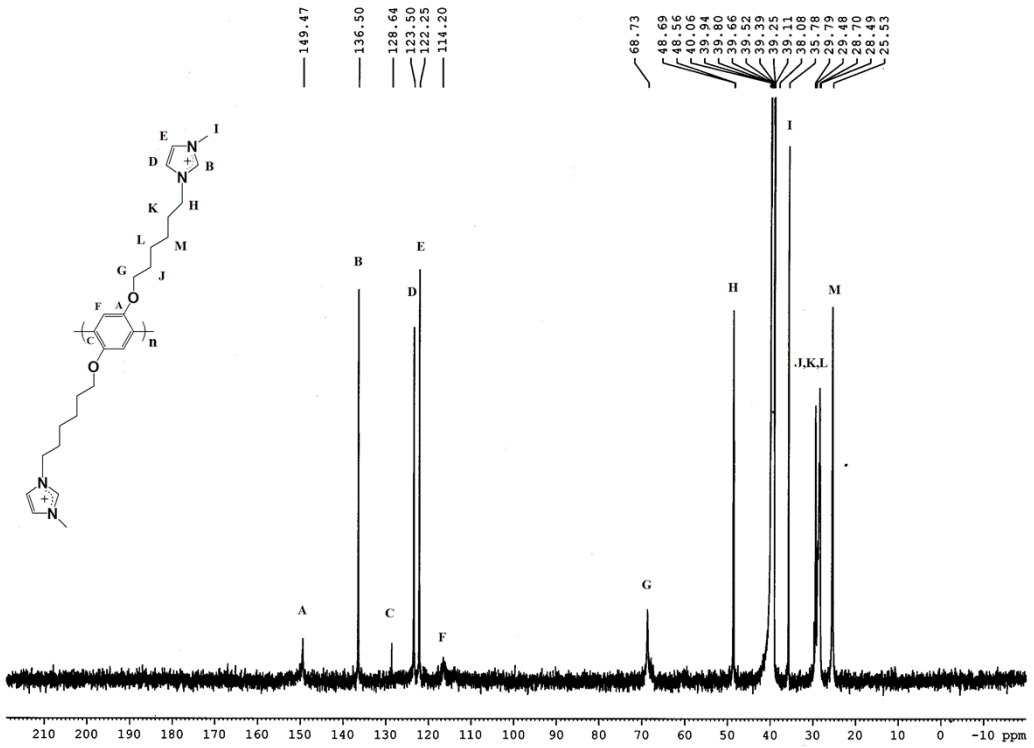

Fig. S2 ^{13}C NMR (150MHz, DMSO-*d6*) spectrum of PMI**.**

Sensing Studies in Aqueous Solution

Stock solution of the polymer PMI and other analytes *viz.* nitrobenzene, nitromethane, benzoic acid, phenol, 4-nitrophenol, 2,4-dinitrophenol were prepared in MilliQ water at concentrations of 1×10^{-3} M and 1×10^{-4} M, respectively. Stock solution of other nitroaromatics *viz.* 2,6-Dinitrotoluene, 2,4-Dinitrotoluene, 4-Nitrotoluene, 1,3-Dinitrobenzene were prepared at concentrations of 1×10^{-4} M, in HPLC grade THF. The absorption measurements and fluorescence titrations of the polymer PMI with different analytes were carried out by sequentially adding 1µL to 3 mL aqueous solution containing 2×10^{-5} M PMI in a quartz cuvette (1 cm × 1 cm). The absorption and fluorescence spectra of the resultant mixtures were then recorded after mixing thoroughly at room temperature.

Calculation of Overlap Integral Values and Förster Radius

To identify the extent of energy transfer, overlap integral values for all analytes were calculated using the equation[5] shown below

$$J(\lambda) = \int_0^\infty F_D(\lambda)\, \varepsilon_A(\lambda)\lambda^4 d\lambda$$

where, $F_D(\lambda)$ denotes the corrected fluorescence intensity of donor in the range of λ to λ + Δλ with the total intensity normalized to unity, ε_A is molar absorptivity of the acceptor at λ in M^{-1} cm^{-1}. The Förster distance R0 was also calculated for PMI-PA interaction using the expression shown below

$$R_0 = 0.211[(J)Q(\eta^{-4})(k^2)]^{1/6}$$

where, J is the degree of spectral overlap between donor fluorescence spectrum and the acceptor absorption spectrum, Q is fluorescence quantum yield of the donor (without acceptor), η is the refractive index of the medium and k^2 is the dipole orientation factor usually taken as 0.667.

Preparation of Fluorescence Test Strips

Test strips were prepared by dip-coating Whattman filter paper (70 mm diameter) in the methanolic solution of PMI (10^{-4} M) followed by removal of solvent in an air stream. PMI coated filter papers were then cut into desired number of pieces (1 cm × 1 cm) and used as solid support for the surface sensing purpose.

Preparation of Fluorescence Film and its Sensing towards PA

In a 50 mL beaker containing PMI (5 mg) and purified chitosan (100 mg), 10 mL Milli-Q water and 100 µL of acetic acid were added followed by continuous stirring for about 15 min to ensure complete dissolution of chitosan. This leads to the formation of highly viscous liquid which was spread on pre-cleaned glass plate/petri dish and dried for 2 hr at 50ºC in vacuum oven. A homogeneous transparent film was obtained that could be easily lifted using forceps for sensing purposes.

For contact mode sensing, 2 mg of PA was rubbed with the left hand thumb, and brushed properly to remove all visible PA particles. Left thumb was then pressed onto the film for 10 sec, kept aside and the impression observed under UV light. Right hand thumb was used as control without using PA. Similar procedure was applied for studying selectivity of the film. 5mg of each solid analyte was rubbed with fingertip and brushed properly to remove all the visible particles before pressing it onto the film. For liquid samples, 2 drops of each analyte were casted on fingertip followed by air drying and pressed onto the film.

Calculation of Detection Limit

For calculating detection limit, different samples of PMI (2×10^{-5} M) each containing PA (0 nM, 5 nM, 10 nM, 15 nM, 20 nM, 25 nM, 30 nM, 35 nM and 40 nM) were prepared separately and fluorescence spectrum was then recorded for each sample by exciting at 325 nm. The detection limit plot for PA was obtained by plotting change in the fluorescence

intensity *vs* the concentration of PA. The curve demonstrates a linear relationship and the correlation coefficient (R^2) *via* linear regression analysis was calculated to be 0.998. The limit of detection (LOD) was then calculated using the equation 3σ/K, where σ denotes the standard deviation for the intensity of PMI in the absence of picric acid and K represents slope of the equation.

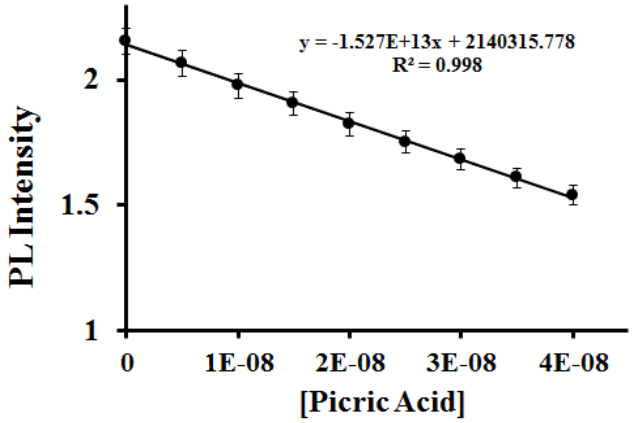

Fig. S3 Fluorescence intensity of PMI (2×10^{-5} M) in aqueous solution as a function of PA concentration.

LOD=3 × S.D./k

LOD = $3 \times 2856.067/1.527 \times 10^{13}$

= 56.11×10^{-11} M (128ppt)

Table S1: A comparative study of the K_{sv}, detection limit and medium used for PA detection of some recent representative reports.

Publication	Material used	K_{sv} (M^{-1})	Detection Limit	Medium Used
Present Manuscript	***Conjugated polyelectrolyte***	***1.0 × 10⁷***	***56.11×10⁻¹¹ M (128 ppt)***	***H_2O***
Angew. Chem. Int. Ed., **2013**, *52*, 2881	Metal-organic framework	3.5×10^4	-	CH_3CN
Chem. Eur. J., **2014**, *20*, 12215	α-cyanostilbene derivative	3.3×10^5	2.8×10^{-7} M	H_2O/THF (v/v=7:3)
Chem. Eur. J. **2014**, 20, 195	Tetraphenylethelene Nanosphere	3.0×10^4	5×10^{-9} M	H_2O/THF (v/v=9:1)

Chem. Mater., **2014**, *26*, 4221	Graphene derivative	8.9×10^5	300 ppb	H_2O/THF (v/v=9:1)
Chem. Commun., **2014**, *50*, 15788	Organic cage	2.2×10^5	6.4 ppb	DCM
ACS Appl. Mater. Interfaces, **2014**, *6*, 10722	Graphene oxide	1.3×10^5	125 ppb	Buffer
ACS Appl. Mater. Interfaces. **2013**, *5*, 5373	Hexa-peri-hexabenzocoronene derivative	3.2×10^6 & 2.0×10^6	4×10^{-9} M & 9×10^{-9} M	H_2O/THF (v/v=4:6)
Inorg. Chem. **2013**, *52*, 4860	Hexaphenylbenzene derivative	1.9×10^5	6.8 ppb	H_2O/THF (v/v=4:6)
ACS Appl. Mater. Interfaces, **2013**, *5*, 672	Pentacenequinone derivative	1.5×10^4	3.5×10^{-7} M	Toluene/DCM (v/v=8:2)
Chem. Commun., **2014**, *50*, 6031	Iridium(III) complex	5.2×10^4	-	H_2O/Acetone (v/v=9:1)
J. Org. Chem. **2013**, *78*, 1306	Tris imidazolium salt	3.8×10^4 & 3.3×10^4	-	DMSO
Chem. Commun., **2012**, *48*, 5007	Fluoranthene derivative	9.9×10^4	20 ppb	Ethanol
ACS Appl. Mater. Interfaces, **2013**, *5*, 8394	*p*-phenylenevinylene derivative	5.5×10^4	1.1×10^{-8}	Brij-58 Micelles

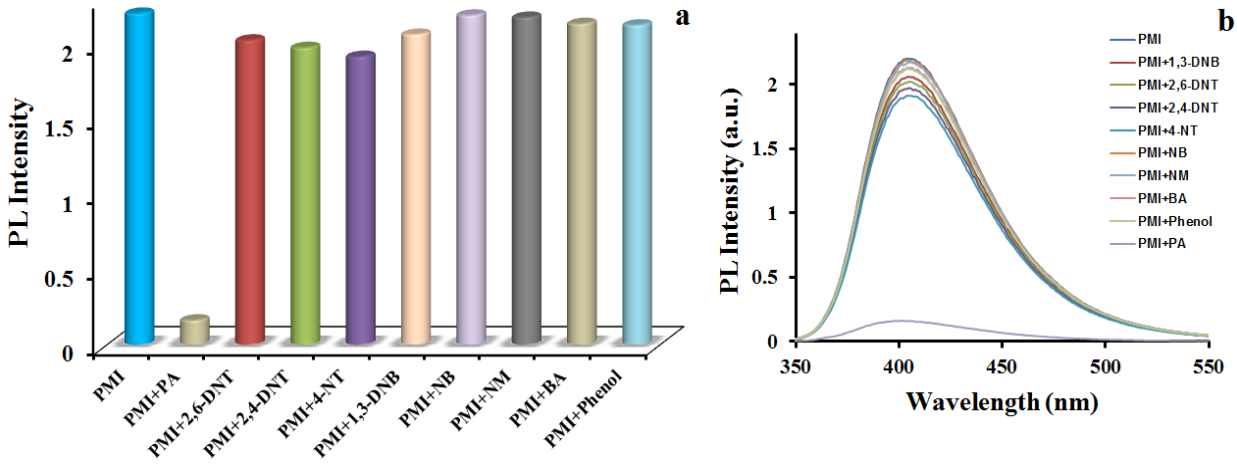

Fig. S4 (a) Bar diagram depicting the effect of various analytes (6.67×10^{-6} M) on fluorescence emission of PMI (2×10^{-5} M) in aqueous media. (b) Corresponding photoluminescence spectra.

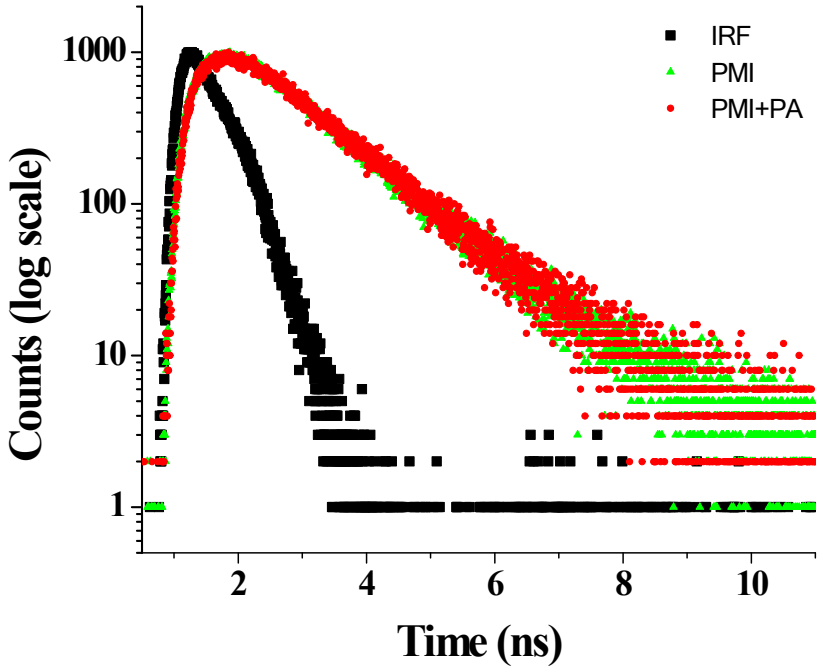

Fig. S5 Lifetime decay profile for PMI with PA (λ_{ex} = 308 nm, monitored at 410 nm).

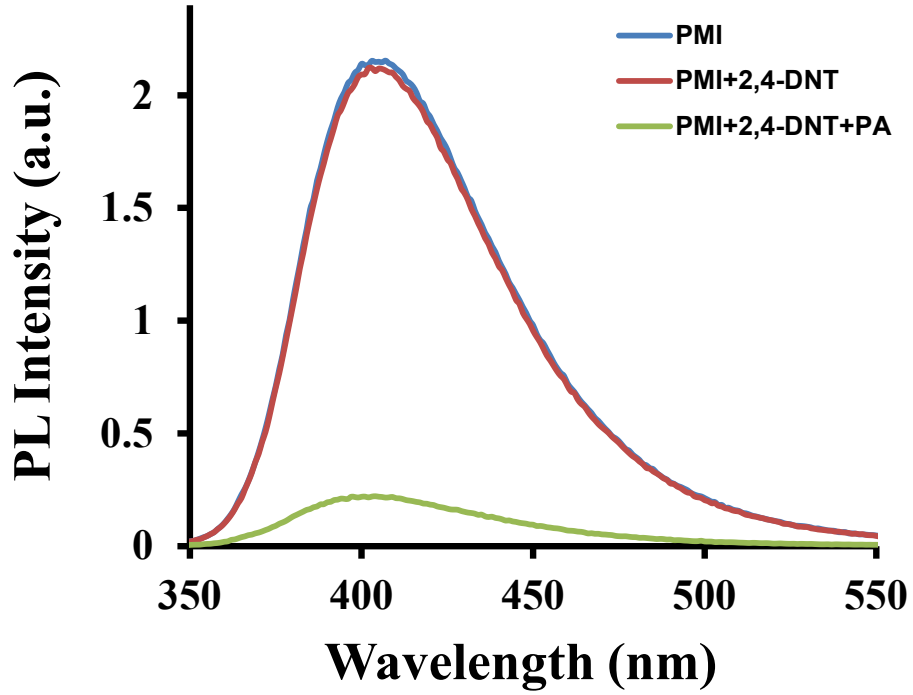

Fig. S6 Change in emission spectra of PMI (2× 10^{-5} M) with 2,4-DNT (6.67 × 10^{-7} M) followed by addition of PA (6.67 × 10^{-7} M).

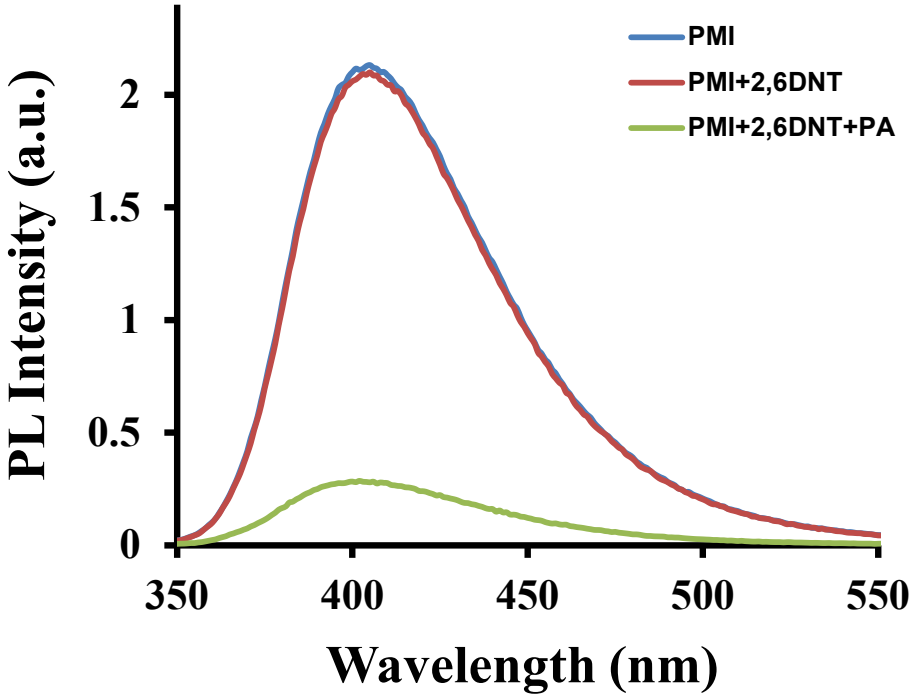

Fig. S7 Change in emission spectra of PMI (2× 10^{-5} M) with 2,6-DNT (6.67 × 10^{-7} M) followed by addition of PA (6.67 × 10^{-7} M).

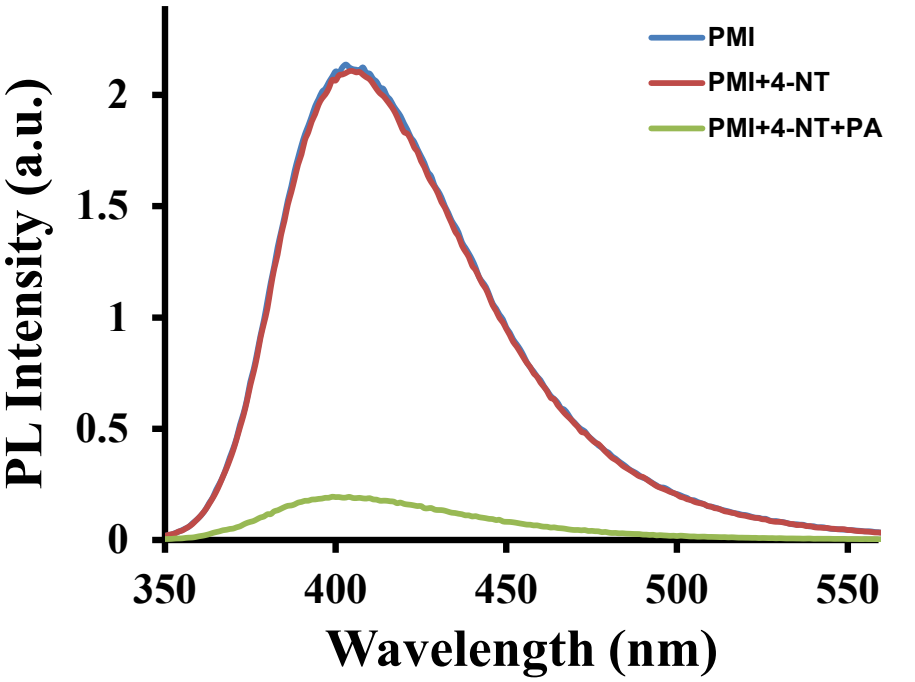

Fig. S8 Change in emission spectra of PMI (2× 10^{-5} M) with 4-NT (6.67 × 10^{-7} M) followed by addition of PA (6.67 × 10^{-7} M).

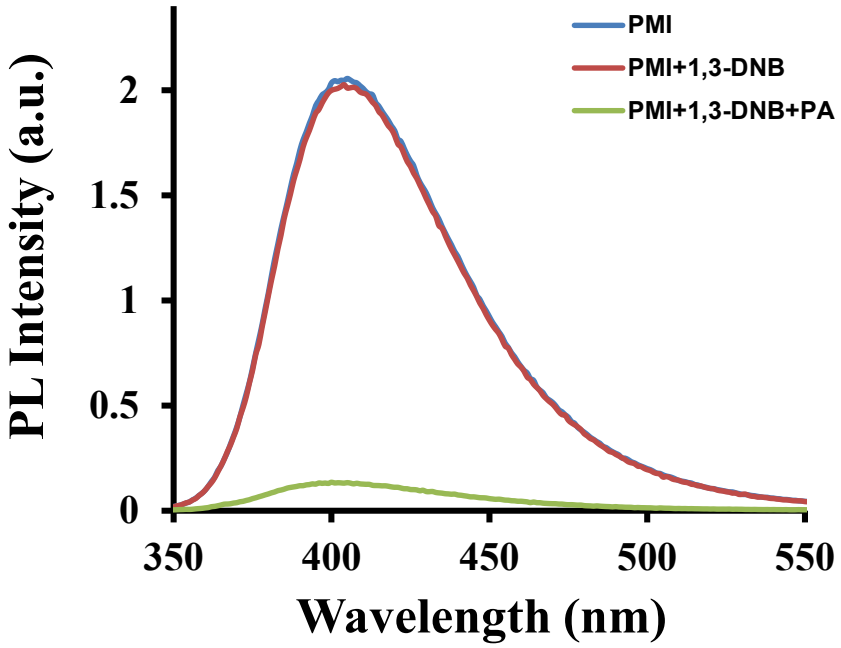

Fig. S9 Change in emission spectra of PMI (2×10^{-5} M) with 1,3-DNB (6.67×10^{-7} M) followed by addition of PA (6.67×10^{-7} M).

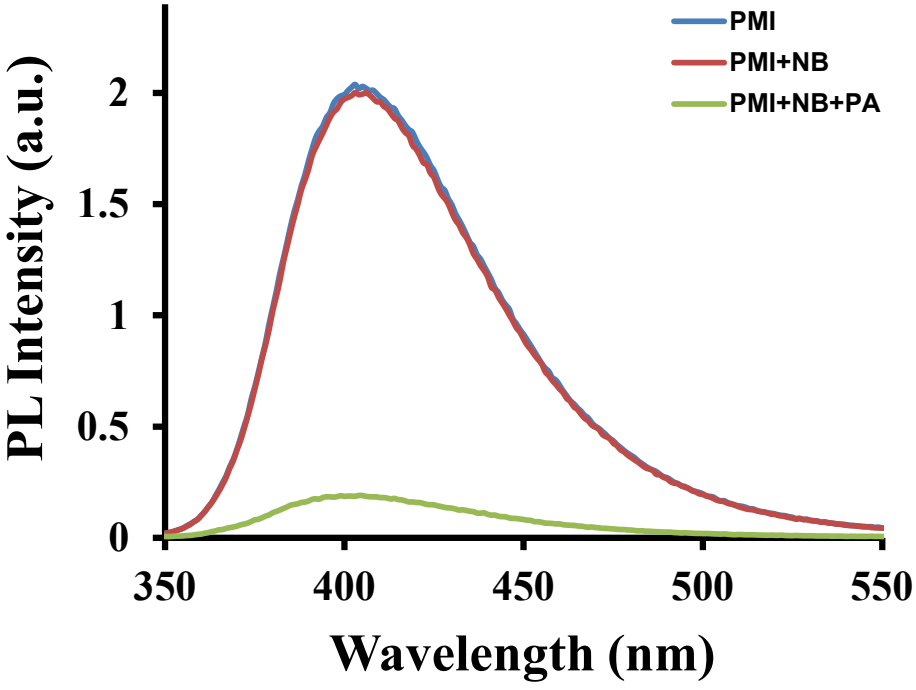

Fig. S10 Change in emission spectra of PMI (2×10^{-5} M) with NB (6.67×10^{-7} M) followed by addition of PA (6.67×10^{-7} M).

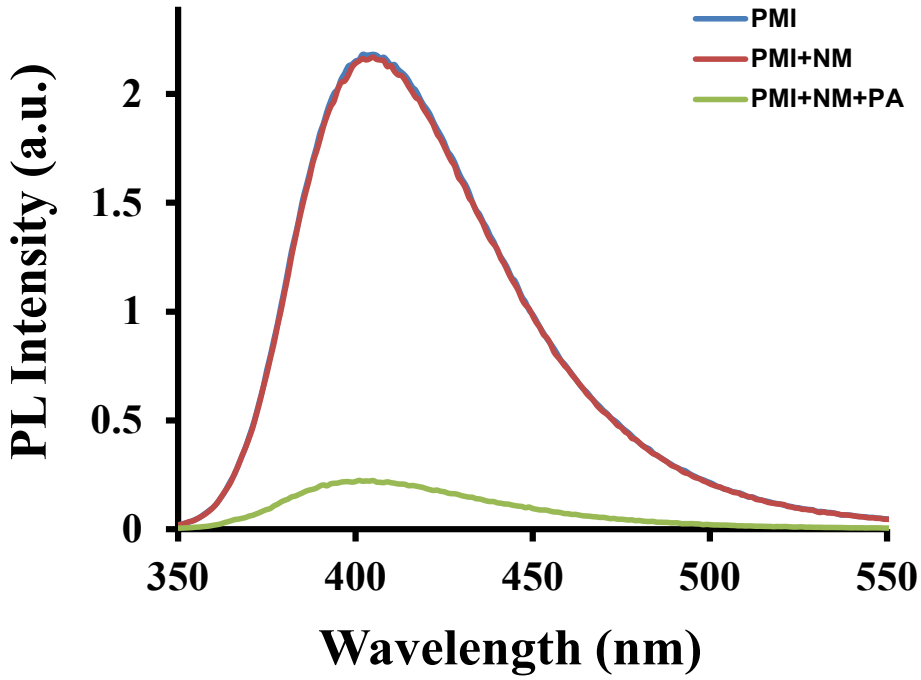

Fig. S11 Change in emission spectra of PMI (2× 10^{-5} M) with NM (6.67 × 10^{-7} M) followed by addition of PA (6.67 × 10^{-7} M).

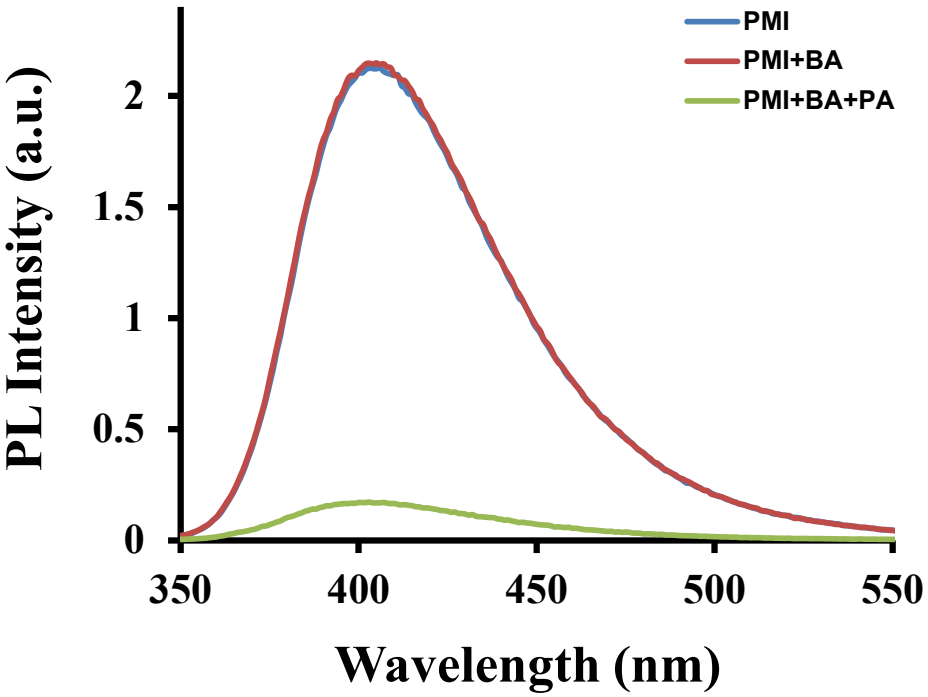

Fig. S12 Change in emission spectra of PMI (2× 10^{-5} M) with BA (6.67 × 10^{-7} M) followed by addition of PA (6.67 × 10^{-7} M).

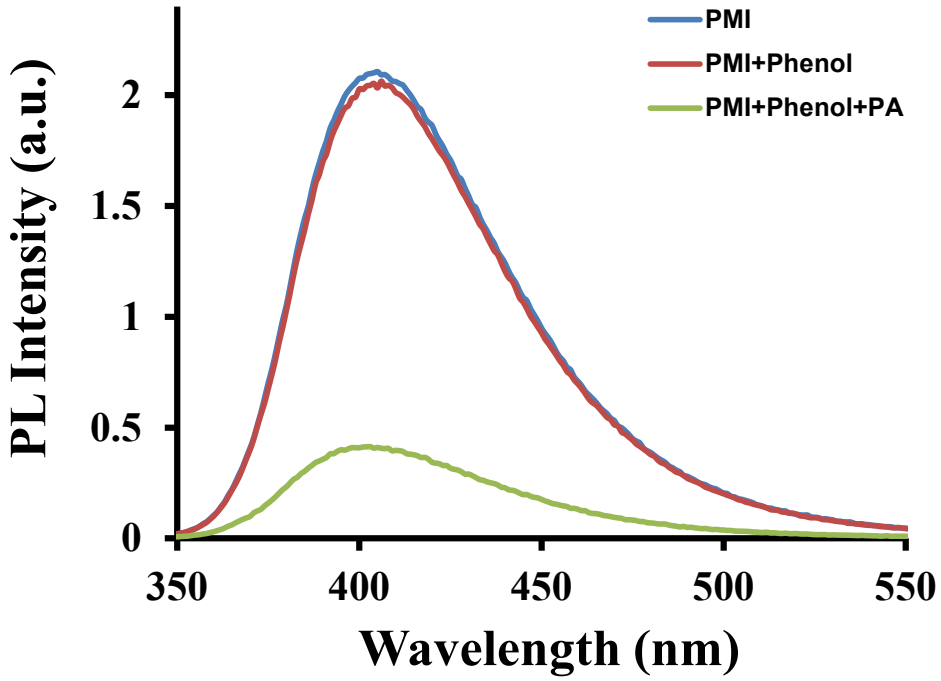

Fig. S13 Change in emission spectra of PMI (2× 10^{-5} M) with Phenol (6.67 × 10^{-7} M) followed by addition of PA (6.67 × 10^{-7} M).

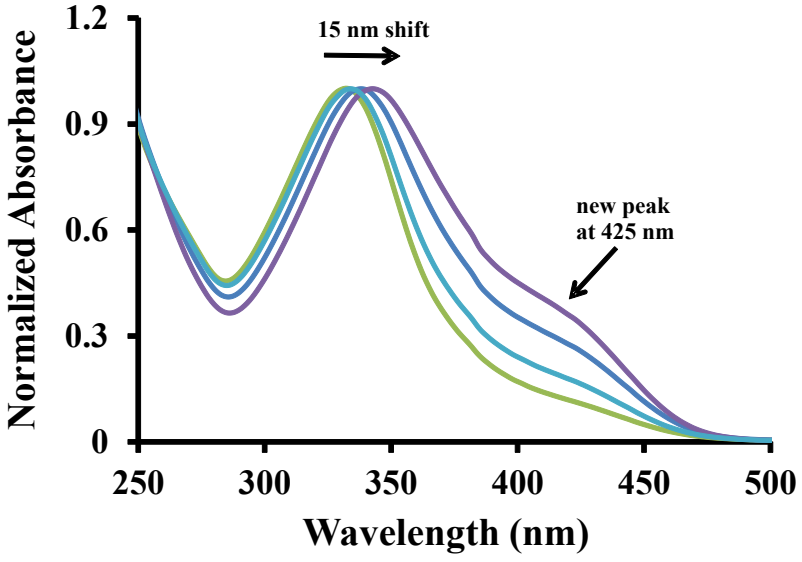

Fig. S14 UV-Vis spectra of PMI upon addition of PA in water. The appearance of new band at 425 nm and red shift in the spectra indicates the formation of ground state complex with PA.

Cyclic Voltammetry

The electrochemical study for PMI was performed using three-electrode cell at room temperature in inert atmosphere using argon. A glassy carbon electrode was used as working electrode. Pt wire and the saturated Ag/Ag^+ electrode were used as counter and reference electrodes, respectively. The Fc^+/Fc couple was used as an internal reference with 0.1M tetrabutylammonium hexafluorophosphate ($TBAPF_6$) as supporting electrolyte in CH_3CN. Noticeable reduction potential was observed for PMI (E_{red} = -0.736V) and LUMO (-4.364eV) energy level was determined through onset calculation according to the method[6] reported for conjugated polymers. The HOMO value calculated by optical energy was found to be -7.674eV.

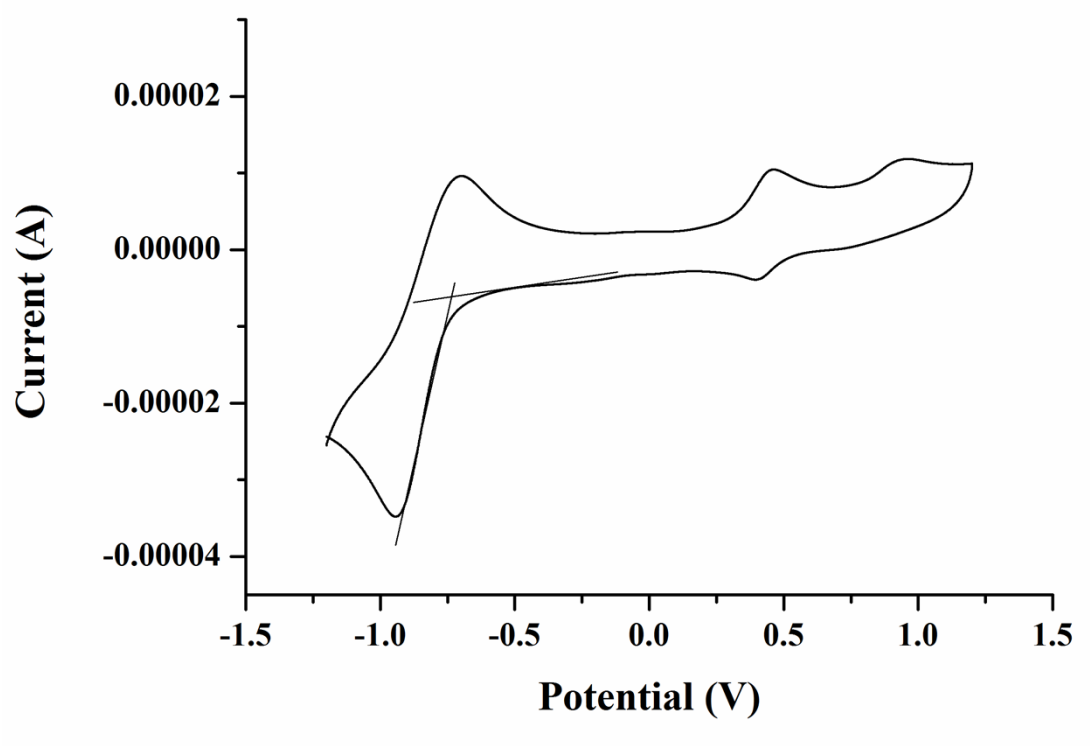

Fig. S15 Cyclic voltammogram of PMI film on glassy carbon electrode in (0.1M) $TBAF_6$, CH_3CN solution with a scan rate of 50 mV/s.

Computational Studies

The monomer of PMI (without two Br^- anions) was used as model to obtain energy optimized structures by density functional theory (DFT) using B3LYP functional and 6-31G basis set in Gaussian 03[7] program. Picric acid, its corresponding picrate ion and various other nitroexplosives have been optimised for the analysis of charge transfer phenomenon.

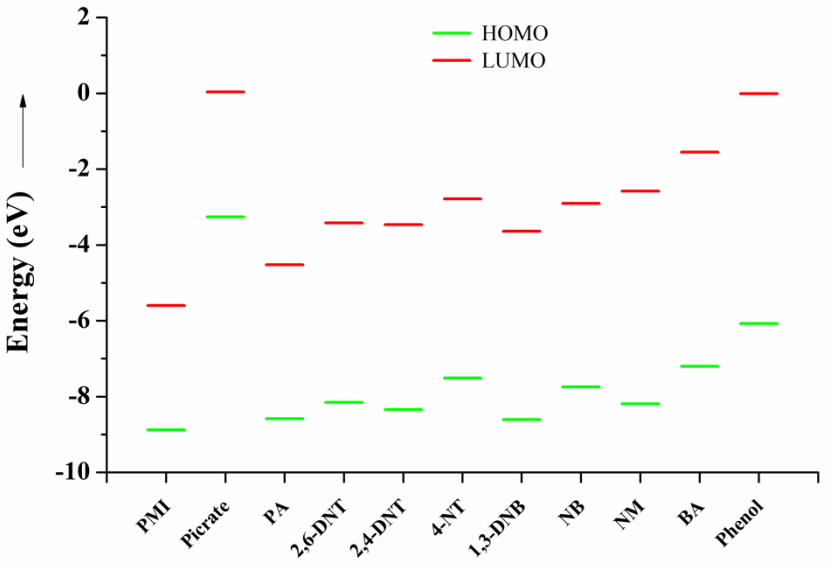

Fig S16. HOMO-LUMO energy levels for PMI and different analytes as calculated by B3LYP/6-31G DFT model.

Table S2. Overlap integral J (λ) values obtained for various analytes

Compounds	**J (λ) values (M^{-1} cm^{-1} nm^4)**
PA	2.63×10^{14}
2,6-DNT	3.90×10^{12}
2,4-DNT	1.54×10^{12}
4-NT	1.98×10^{12}
1,3-DNB	5.16×10^{12}
NB	4.86×10^{12}
NM	8.32×10^{12}
BA	1.30×10^{12}
Phenol	6.24×10^{12}

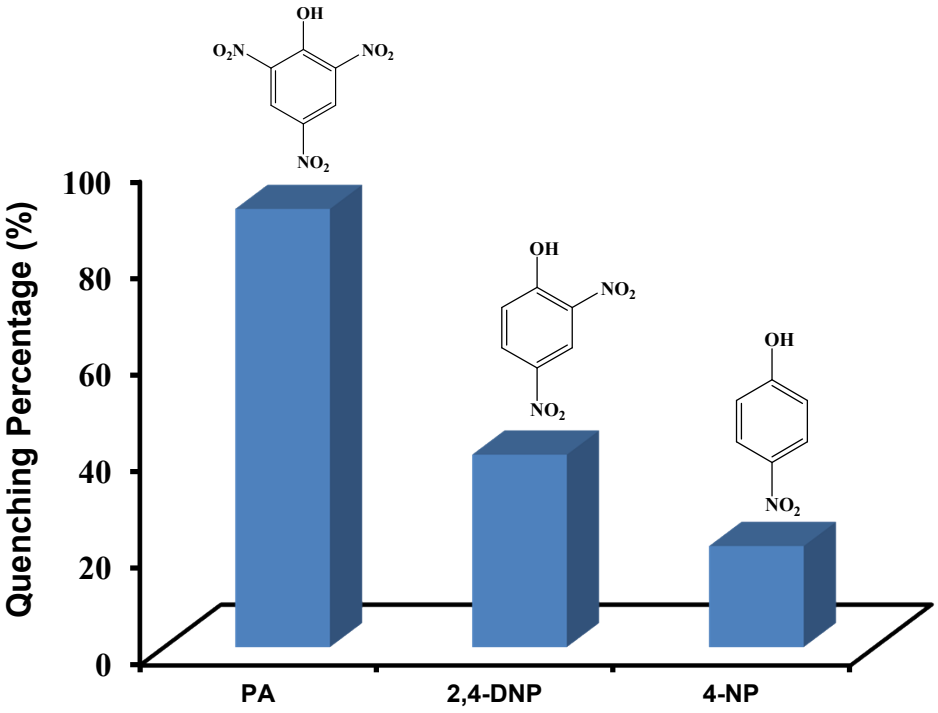

Fig. S17 Comparison of percentage fluorescence quenching obtained on addition of PA, 2,4-DNP and 4-NP to the solution of PMI in water. Concentration of PMI and each analyte were 2×10^{-5} M and 6.67×10^{-7} M, respectively.

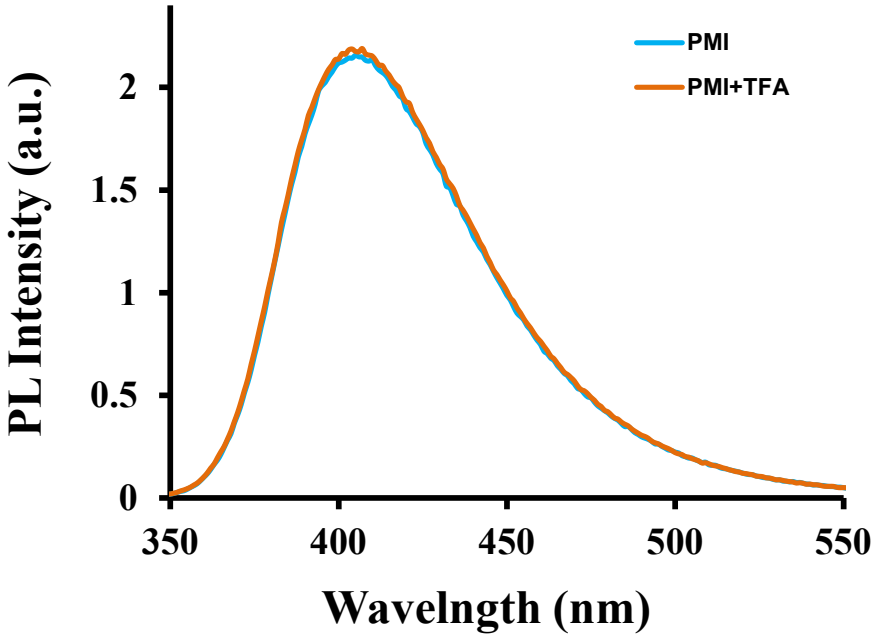

Fig. S18. Change in emission spectra of PMI (2×10^{-5} M) after adding TFA (1×10^{-6} M) in aqueous media.

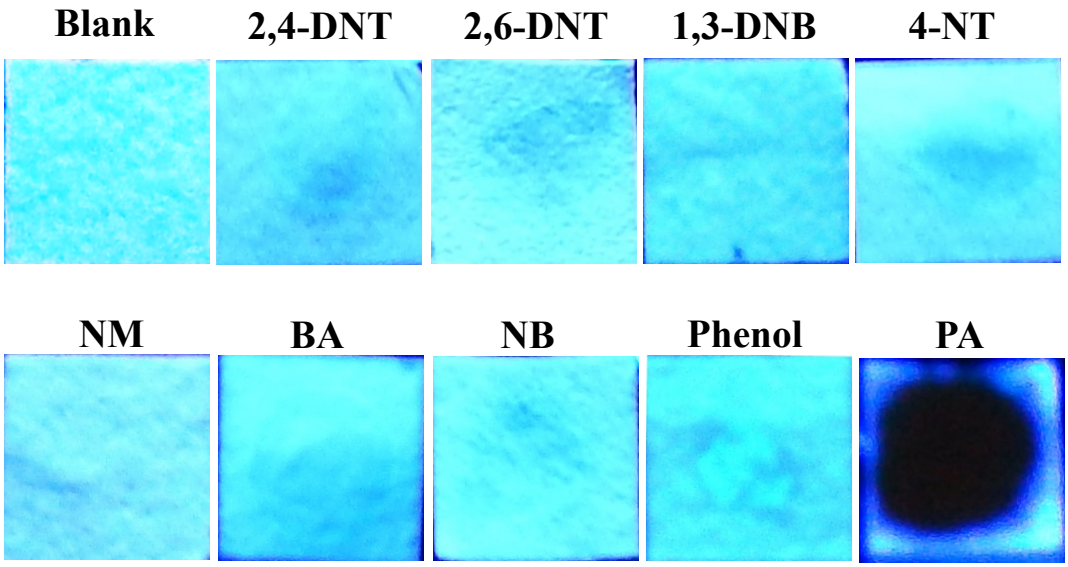

Fig. S19 Colour of fluorescent test strips under UV light before and after addition (10μL) of 10^{-2} M solution of various analytes.

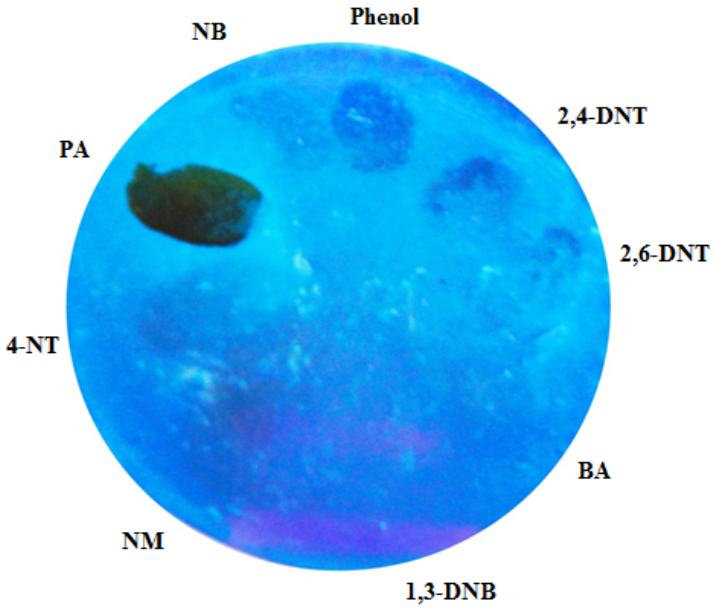

Fig. S20 Visualization of PMI-doped CS fluorescent film under UV light with fingertip impression of different analytes.

Optimized coordinates of PMI

Center Number	Atomic Number	Atomic Type	Coordinates (Angstroms) X	Y	Z
1	6	0	-1.289473	-0.031433	-0.528791
2	6	0	-0.649594	-1.259685	-0.326775
3	6	0	0.646319	-1.287314	0.196771
4	6	0	1.289820	-0.086571	0.517461
5	6	0	0.650053	1.141641	0.315278
6	6	0	-0.646013	1.169258	-0.208062
7	1	0	-1.162853	-2.176949	-0.593015
8	1	0	1.156779	-2.227768	0.371893
9	1	0	1.163117	2.059051	0.581427
10	1	0	-1.156319	2.109844	-0.382998
11	8	0	2.575134	-0.117100	1.094774
12	8	0	-2.574986	-0.001981	-1.105691
13	6	0	3.709551	-0.077885	0.165700
14	1	0	3.656849	-0.937794	-0.517062
15	1	0	3.661334	0.840384	-0.436600
16	6	0	4.972662	-0.120049	1.018234
17	1	0	4.953971	0.734017	1.707220
18	1	0	4.941443	-1.025792	1.637240
19	6	0	6.262801	-0.096295	0.178105
20	1	0	6.270403	-0.952153	-0.512941
21	1	0	6.282736	0.809451	-0.445828
22	6	0	7.529700	-0.139064	1.054433
23	1	0	7.521027	0.717854	1.743610
24	1	0	7.505527	-1.043299	1.679868
25	6	0	8.830094	-0.120987	0.225898
26	1	0	8.841158	-0.976807	-0.462509
27	1	0	8.868104	0.786718	-0.391033
28	6	0	10.068687	-0.174166	1.134577
29	1	0	10.096922	0.684954	1.810830

30	1	0	10.068536	-1.078957	1.749533
31	6	0	-3.708966	-0.040398	-0.176032
32	1	0	-3.657634	0.821553	0.504195
33	1	0	-3.658682	-0.956844	0.428941
34	6	0	-4.972603	-0.004084	-1.028060
35	1	0	-4.951568	0.906508	-1.640346
36	1	0	-4.944508	-0.852777	-1.723337
37	6	0	-6.262174	-0.049504	-0.187960
38	1	0	-6.281083	0.801207	0.509131
39	1	0	-6.269822	-0.959876	0.429556
40	6	0	-7.529807	-0.018497	-1.063730
41	1	0	-7.523728	0.895081	-1.675904
42	1	0	-7.504273	-0.864931	-1.765310
43	6	0	-8.829315	-0.076252	-0.235614
44	1	0	-8.867293	0.771745	0.461097
45	1	0	-8.838803	-0.990931	0.372496
46	6	0	-10.069021	-0.047910	-1.143891
47	1	0	-10.062772	-0.886472	-1.846441
48	1	0	-10.105225	0.874477	-1.730500
49	7	0	-11.345648	-0.129524	-0.381622
50	6	0	-12.163793	0.904489	-0.098851
51	6	0	-11.873665	-1.285660	0.192639
52	1	0	-12.020582	1.924574	-0.411050
53	6	0	-13.032396	-0.928822	0.827322
54	1	0	-11.393230	-2.243896	0.097859
55	1	0	-13.740797	-1.519536	1.382107
56	7	0	11.346784	-0.168605	0.370443
57	6	0	12.154809	0.896104	0.191631
58	6	0	11.886925	-1.257851	-0.313001
59	1	0	12.001218	1.879245	0.602016
60	6	0	13.042360	-0.829059	-0.908005
61	1	0	11.416069	-2.225491	-0.313218
62	1	0	13.757073	-1.355586	-1.516709

63	7	0	-13.197799	0.442709	0.635365
64	7	0	13.193925	0.518663	-0.582420
65	6	0	-14.329241	1.246985	1.140165
66	1	0	-15.259248	0.896833	0.688340
67	1	0	-14.385745	1.156156	2.226281
68	1	0	-14.171011	2.292385	0.875195
69	6	0	14.318006	1.379548	-1.003260
70	1	0	15.250561	0.997357	-0.583788
71	1	0	14.378305	1.394310	-2.092852
72	1	0	14.147684	2.392856	-0.639517

Optimized coordinates of picrate

Center Number	Atomic Number	Atomic Type	Coordinates (Angstroms) X	Y	Z
1	6	0	-0.571700	-1.231579	-0.000042
2	6	0	0.807625	-1.216591	0.000012
3	6	0	1.501818	-0.000098	0.000046
4	6	0	0.807783	1.216486	0.000045
5	6	0	-0.571539	1.231653	0.000004
6	6	0	-1.400198	0.000091	-0.000122
7	1	0	1.350805	-2.150897	0.000043
8	7	0	2.933134	-0.000191	0.000112
9	7	0	-1.184602	2.548924	0.000066
10	7	0	- 1.184936	-2.548769	-0.000032
11	8	0	-2.654124	0.000172	-0.000147
12	8	0	-2.442360	2.669008	0.000304
13	8	0	3.547080	-1.119924	-0.000045
14	8	0	-0.408401	-3.570622	-0.000037
15	8	0	3.547225	1.119462	-0.000010
16	8	0	-2.442710	-2.668687	0.000118
17	8	0	-0.407933	3.570674	-0.000286
18	1	0	1.351086	2.150721	0.000096

Optimized coordinates of picric acid

Center Number	Atomic Number	Atomic Type	Coordinates (Angstroms) X	Y	Z

1	6	0	0.572349	-1.184898	-0.009717
2	6	0	-0.819827	-1.256628	0.018951
3	6	0	-1.546951	-0.076117	0.021583
4	6	0	-0.917302	1.170854	0.001065
5	6	0	0.466951	1.231065	-0.001214
6	6	0	1.267381	0.060771	-0.021674
7	1	0	-1.317540	-2.217189	0.032379
8	7	0	-3.009254	-0.138479	0.042913
9	7	0	1.071361	2.570342	0.013872
10	7	0	1.307567	-2.437524	-0.033071
11	8	0	2.601735	0.167551	-0.087213
12	1	0	3.016189	-0.742717	-0.111737
13	8	0	2.174640	2.726423	0.593387
14	8	0	-3.546470	-1.280711	0.052253
15	8	0	0.675038	-3.518581	0.000904
16	8	0	-3.640226	0.954373	0.051183
17	8	0	2.590885	-2.387249	-0.089001
18	8	0	0.403996	3.493953	-0.537085
19	1	0	-1.498755	2.083176	-0.016042

References:

1. G. S. Paul, P. J. Sarmah and P. K. Iyer, P. Agarwal, *Macromol. Chem. Phys*. 2008, **209**, 417-423.
2. A. J. J. M. van Breemen, P. T. Herwig, C. H. T. Chlon, J. Sweelssen, H. F. M. Schoo, E. M. Benito, D. M. de Leeuw, C. Tanase, J. Wildeman and P. W. M. Blom, *Adv. Funct. Mater.* 2005, **15**, 872-876.
3. G. Saikia, R. Singh, P. J. Sarmah, M. W. Akhtar, J. Sinha, M. Katiyar and P. K. Iyer, *Macromol. Chem. Phys*. 2009, **210***,* 2153-2159.
4. S. Hussain, A. H. Malik and P. K. Iyer, *ACS Appl. Mater. Interfaces,* 2015, **7**, 3189-3198.
5. J. R. Lakowicz, *Principles of Florescence spectroscopy*, 3rd ed; Springer: Singapore, **2010**; pp 443−472.
6. C.M. Cardona, W. Li, A. E. Kaifer, D. Stockdale and G. C. Bazan, *Adv. Mater*. 2011, **23**, 2367-2371.
7. Gaussian 03, Revision E.01, M. J. Frisch, G. W. Trucks, H. B. Schlegel, G. E. Scuseria, M. A. Robb, J. R. Cheeseman, J. A. Montgomery, Jr., T. Vreven, K. N. Kudin, J. C. Burant, J. M. Millam, S. S. Iyengar, J. Tomasi, V. Barone, B. Mennucci, M. Cossi, G. Scalmani, N. Rega, G. A. Petersson, H. Nakatsuji, M. Hada, M. Ehara, K. Toyota, R. Fukuda, J. Hasegawa, M. Ishida, T. Nakajima, Y. Honda, O. Kitao, H. Nakai, M. Klene, X. Li, J. E. Knox, H. P. Hratchian, J. B. Cross, V. Bakken, C. Adamo, J. Jaramillo, R.

Gomperts, R. E. Stratmann, O. Yazyev, A. J. Austin, R. Cammi, C. Pomelli, J. W. Ochterski, P. Y. Ayala, K. Morokuma, G. A. Voth, P. Salvador, J. J. Dannenberg, V. G. Zakrzewski, S. Dapprich, A. D. Daniels, M. C. Strain, O. Farkas, D. K. Malick, A. D. Rabuck, K. Raghavachari, J. B. Foresman, J. V. Ortiz, Q. Cui, A. G. Baboul, S. Clifford, J. Cioslowski, B. B. Stefanov, G. Liu, A. Liashenko, P. Piskorz, I. Komaromi, R. L. Martin, D. J. Fox, T. Keith, M. A. Al-Laham, C. Y. Peng, A. Nanayakkara, M. Challacombe, P. M. W. Gill, B. Johnson, W. Chen, M. W. Wong, C. Gonzalez, and J. A. Pople, Gaussian, Inc., Wallingford CT, **2004**.